

Dynamic characterization for the dielectric electroactive polymer fundamental sheet

Yousef Iskandarani · Hamid Reza Karimi

Received: 16 January 2012 / Accepted: 24 July 2012
© Springer-Verlag London Limited 2012

Abstract A study into the appropriateness of characterizing the dynamics of the dielectric electroactive polymer (DEAP) fundamental sheet has been performed. Whereby a model describing the dynamics of the DEAP fundamental sheet is developed, parameters of the models are determined using experimental/simulation results, and verification has been conducted to determine the precision of the dynamic model. The precision for the DEAP sheet-obtained dynamic model could not be verified unless some parameters characterizing the material properties are found. For this purpose, a set of preparatory experiments are done in order to find the material properties “Young’s modulus and damping”. The testing for finding the material properties is requested before doing the dynamic analysis; both material characterization and dynamic analysis tests are performed using the developed testing rig which will be described in the paper. The results of this study highlight the dependency of the material dynamics on the mechanical fixture of the material, whereby the range of operation can be reduced to lower frequencies or expanded to higher frequencies when the mechanical fixture is designed for a certain application. The test results for the material show a relatively visible error between 0 and 20 Hz, but the error diverges after this range was stimulated when exceeding the natural frequency of the system, leading to non-stable state affecting the controllability of the actuated

material. The following error is established due to the static friction in the setup and mainly as expected before the ignorance of the polymer creep, as exhibited through the dynamic experimentation verified by an excellent correlation whenever viscoelastic property is considered.

Keywords Characterization · DEAP · Dynamic analysis · Dynamic range · Modeling · Simulation · Testing rig · Working principles

1 Introduction to Electro Active Polymers

Electroactive polymers (EAP) are able to change size and/or shape when submitted to electrical stimulation. There are two types: ionic and electronic. The ionic types work by using ion exchange between two electrodes when a DC-voltage source is applied: the ions are transported from the positive electrode to the negative one in the solution between them, causing a swelling in one side and a shrinking in the other; see for instance [1–3].

Respectively, the pros and cons are large bending displacements with the application of low voltages, but the response is very slow and with a low actuation force. The electronic types of EAP utilize two forces:

1. The Maxwell forces between two electrodes where a high-voltage direct current source is applied, creating opposite electrical charges that attract each other. This attraction between the charged electrodes squeezes the soft but noncompressible polymer in the middle, causing it to expand in the

Y. Iskandarani · H. R. Karimi (✉)
Department of Engineering, University of Agder,
Grimstad, Norway
e-mail: hamid.r.karimi@uia.no

Y. Iskandarani
e-mail: yousef.iskandarani@uia.no

directions orthogonal to the applied pressure, as shown in Fig. 1.

- The electrostrictive forces [4] are created when randomly aligned electrical polarized molecules or dipoles within the dielectric material (Fig. 2a) are subjected to an electric field: the opposite sides of the domains become differently charged and attract each other (Fig. 2b), reducing material thickness in the direction of the applied field from within the material [5], like the Maxwell forces do from the surface [4].

The electronic EAP element can be considered as a variable capacitor, which gives it a major advantage in being able to hold the actuator strain when the electrical charge stays on the electrodes. It can also function as a sensor where applied mechanical work changes its capacitance, but the disadvantage is the high voltage required to strain it [6–8].

Comparatively, EAPs can be seen to have many advantages for actuation and a large range of dynamic response: low power consumption along with the ability to hold strain when not activated, high-energy density [9], and large flexibility at low forces are extremely desirable properties for its potential use in many core electromechanical applications [10, 11]. A large potential also exists for using EAP for creating new technologies and new market areas [12], of which one of these areas is energy harvesting, as a feasibility study have

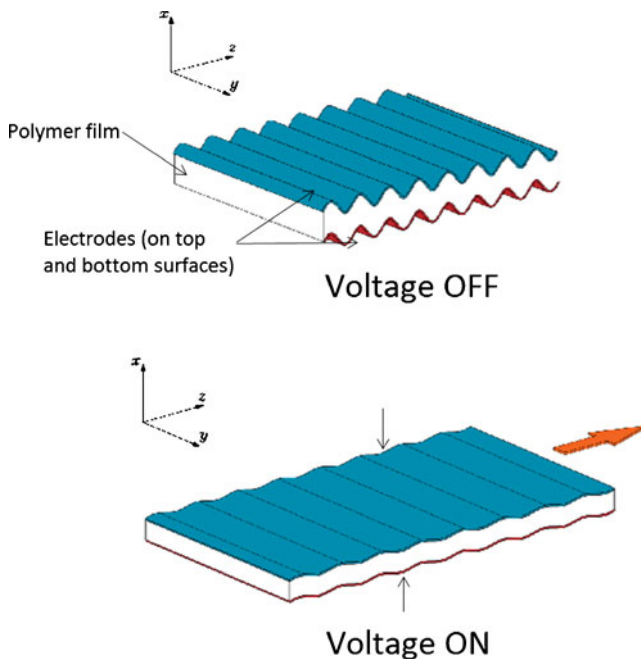


Fig. 1 Applying voltage to the electrodes makes the electronic EAPs change their shape

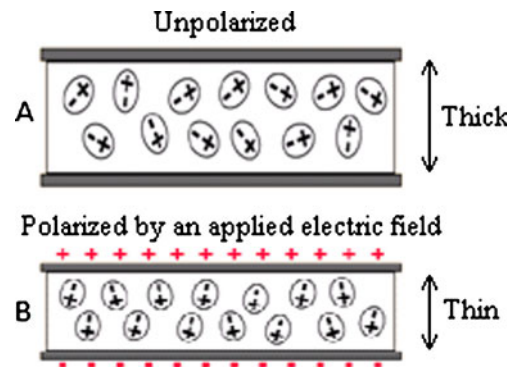


Fig. 2 With an electric field aligning the dipoles in the dielectricum, the electrostrictive forces pulls the material together

shown that the DEAP is a candidate with many value propositions over other smart materials [13].

In the case of the DEAP material, as the one used in this work, the electrostrictive forces from polarized molecules are not applicable to this material and not a significant force to be considered. Of course, in each dielectric material, there will be polarization effects in an electric field. But here, the effect of motion from these small charges is negligible compared to the attractive forces from the electrodes.

In the following work, the dielectric EAP developed by Danfoss PolyPower A/S is used. Danfoss PolyPower is a leading company in the area of EAP which is based in Nordborg, Denmark. Since this paper focus on actuators made of PolyPower, the focus in the rest of the paper will be only on dielectric EAP (PolyPower DEAP).

2 Static working principles

Before doing a dynamic analysis, the static analysis is studied in order to understand the working principles of the DEAP material. For this purpose, a three-dimensional building block representing the particle scale of the material is introduced, as shown in Fig. 3. Also, it can give some idea to determine some of the constants experimentally since it is usually more simple to do static than dynamic experiments.

The DEAP actuator consists of two surfaces of compliant electrodes with a rubber-like material “elastomer” in between. Initially, the behavior of the DEAP material will be explained when the high voltage is applied across the electrodes.

As a result of the induced voltage across the DEAP electrodes, the Maxwell stress is given by

$$\sigma_m = \epsilon_r \epsilon_0 E^2 \quad (1)$$

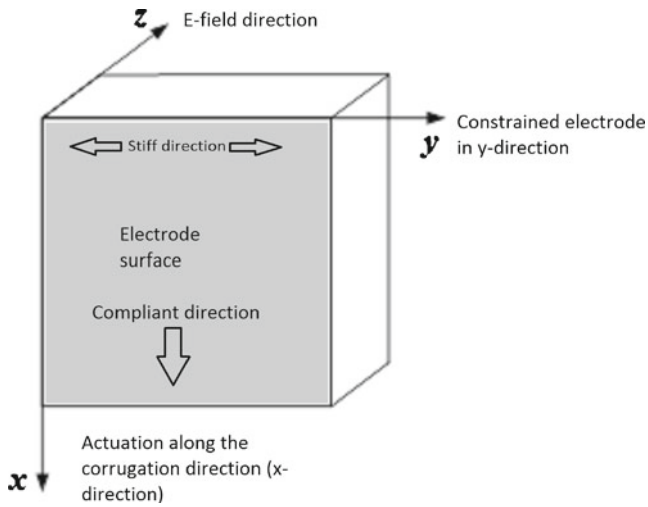


Fig. 3 Fundamental DEAP particle representation in three dimensions

where ϵ_r and ϵ_0 are the relative and absolute permittivity, σ_m is the stress, and E is the electric field.

The unique corrugation of the PolyPower material creates a slightly more complex geometry which will be resulting more complex electromechanical response. However, for simplifying the modeling work assuming a negligible height of the corrugation relative to the material thickness, the relation for a plate capacitor with uniform electric field will be used. The voltage difference between the plates can be found by

$$E = \frac{u}{z} \tag{2}$$

where z is the dielectric thickness

So the Maxwell stress on the plates, related to a voltage applied on the electrodes, is given by

$$\sigma_m = \epsilon_r \epsilon_0 \left(\frac{u}{z}\right)^2 \tag{3}$$

If the material between the electrodes is incompressible, the volume conservation can be stated as follows:

$$V_0 = V \rightarrow x_0 y_0 z_0 = xyz \tag{4}$$

where V_0 is the initial volume and V is the final volume, and x_0 , y_0 , and z_0 are the initial length, width and thickness respectively. Hence, x , y , and z are the final length, width, and thickness, respectively.

One of the main properties of the PolyPower DEAP material is the fact that it is constrained in the y -direction, so that $y_0 = y$ and Eq. 4 reduce to

$$x_0 z_0 = xz \tag{5}$$

defining the stretch ratio α as

$$\alpha = \frac{x}{x_0} = \frac{z_0}{z} \tag{6}$$

Inserting this into Eq. 3 yields

$$\sigma_m = \epsilon_r \epsilon_0 \left(\frac{u}{\frac{z_0}{\alpha}}\right)^2 = \epsilon_r \epsilon_0 \alpha^2 \frac{u^2}{z_0^2} \tag{7}$$

If the elongation in the x -direction is defined as

$$\Delta x = x - x_0, \tag{8}$$

then the stretch ratio can be expressed with

$$\alpha = \frac{\Delta x}{x_0} + 1 \tag{9}$$

and the equation in more general expression can be found when inserting Eq. 9 in Eq. 7

$$\sigma_m = \epsilon_r \epsilon_0 \left(\frac{\Delta x}{x_0} + 1\right)^2 \frac{u^2}{z_0^2} \tag{10}$$

Hooke's law states that

$$\sigma = Ye \tag{11}$$

where Y is the Young's modulus and e is the strain defined as

$$e = \alpha - 1 \tag{12}$$

which, by the definition in Eq. 8, can as well be written as follows:

$$e = \frac{\Delta x}{x_0} \tag{13}$$

So the Hooke's law can be written as

$$\sigma = Y \frac{\Delta x}{x_0} \tag{14}$$

Equation 10 is the Maxwell stress in the z -direction, and Eq. 14 is the Hookean material stress in the x -direction. So, Eqs. 10 and 14 are used together assuming the same value of stress to get the relation between the applied voltage (input) and the elongation (output) in the x -direction:

$$\frac{\Delta x}{x_0} \frac{1}{\left(\frac{\Delta x}{x_0} + 1\right)^2} = \frac{\epsilon_r \epsilon_0}{z_0^2 Y} u^2 \tag{15}$$

For low strains, the quadratic relation between the voltage and the strain can be approximated to

$$\frac{\Delta x}{x_0} \approx \frac{\epsilon_r \epsilon_0}{z_0^2 Y} u^2 \tag{16}$$

2.1 Electrical modeling

The DEAP material can be described as RCL network, meaning that the material have resistance, inductance, and capacitance. In order to charge the DEAP material, some power electronics are needed. These electronics are being developed with regards to the size of the actuator which can be represented by its capacitance. In principle, when driving a high-voltage power supply, certain safety measures have to be taken into account. A high voltage power supply (HVPS) is used to charge up the EAP actuated material. The amount of charge per time—the watts—has to be determined in order to know the possibilities of a quick response. Normal HVPS can supply between 1–20 Watts at 2.5 kV.

It is customary to model the DEAP material as in Fig. 4a where a resistive element, infinite resistive element, can be added in parallel to the capacitance if there is no leakage; but for simplicity, the model on Fig. 4b will be used. To model that, the expression of the capacitance potential will be used as shown in Eqs. 17, 18, and 19.

The potential of the capacitance can be found as follows:

$$\frac{1}{C} \int I(t)dt = u(t). \tag{17}$$

The current can be describe as a function of charge:

$$I(t) = \frac{dq}{dt}. \tag{18}$$

Insert Eq. 18 in Eq. 17 and solve to get the relation between the charge and potential:

$$\frac{1}{C}q = u(t). \tag{19}$$

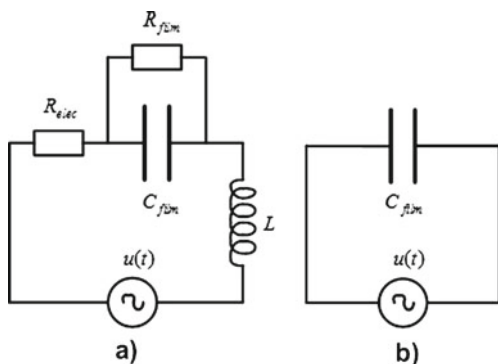


Fig. 4 DEAP material electrical model showing **a** customary model and **b** the used simpler model

3 Dynamic modeling

3.1 Mechanical modeling

The mechanical model of the material is rather very simple, but it is important to derive, as some assumption are considered. For such a system, Hooke’s law states the following:

$$\sigma_{Hooke} = Ye. \tag{20}$$

The strain as a function of stretch ration is defined by

$$e = \alpha - 1, \tag{21}$$

introducing the mechanical stress as

$$\sigma_{Hooke} = Y(\alpha - 1), \tag{22}$$

incompressible material and constrained in the y-direction \Rightarrow

$$\alpha = \frac{x}{x_0} = \frac{z_0}{z}. \tag{23}$$

3.2 Electromechanical modeling

The Maxwell stress is given by

$$\sigma_m = \epsilon_r \epsilon_0 \left(\frac{u_c}{z} \right)^2. \tag{24}$$

The capacitance is dependent on the geometry and the material between the electrodes, hence given by the following:

$$C = \epsilon_r \epsilon_0 \frac{A}{z} \Leftrightarrow \epsilon_r \epsilon_0 = \frac{Cz}{A} \tag{25}$$

where A is the area of the capacitance. Insert in Eq. 24 to get

$$\sigma_m = \frac{Cz}{A} \left(\frac{u}{z} \right)^2 = \frac{Cu^2}{Az} = \frac{Cu^2}{V} \tag{26}$$

u is discarded, and the charge q is used instead as the coupling variable between the electrical and the mechanical model. So,

$$u = \frac{q}{C}. \tag{27}$$

To rewrite Eq. 26 as

$$\sigma_m = \frac{q^2}{CV} \tag{28}$$

from Eq. 25, the expression of the capacitance is found:

$$C \propto \frac{A}{z} = \frac{yx}{z} = \frac{yx_0\alpha}{\frac{z_0}{\alpha}} = \frac{yx_0}{z_0}\alpha^2 \quad (29)$$

and approximated as

$$C = C_0\alpha^2. \quad (30)$$

Finally, the Maxwell stress becomes

$$\sigma_m = \frac{q^2}{C_0\alpha^2V} = \frac{1}{C_0V}\frac{q^2}{\alpha^2}. \quad (31)$$

3.3 The governing equations

The DEAP sheet is modeled as spring–mass–damper system, as shown on Fig. 5. It is highly important to highlight that the following model represent a free-hanging sheet with a mass; so, the friction component is not considered because, in principle, it should not be there, but it would appear that the friction influence the system and its behavior, creating high losses in the strain due to the LVDT which is placed in contact with the system. Apply Newton’s 2nd Law on the mass for determining the governing equations as follows:

$$m\frac{d^2x}{dt^2} = f_g - f_{viscous} - f_{spring} + f_{maxwell} \quad (32)$$

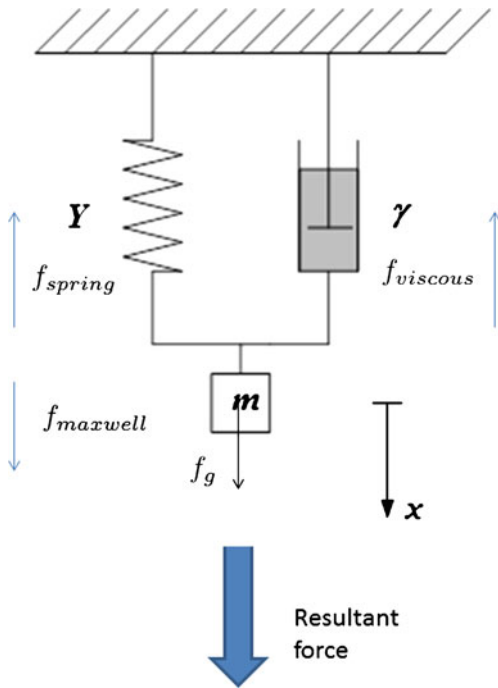


Fig. 5 DEAP material system model

where f_g is the gravity force:

$$f_g = mg \quad (33)$$

and $f_{viscous}$ is the force due to friction from the dash pot with constant damping coefficient γ :

$$f_{viscous} = \gamma \frac{dx}{dt} = \gamma x_0 \frac{d\alpha}{dt}. \quad (34)$$

In order to determine the spring force f_{spring} due to the stress, where A is the cross-sectional area, it is assumed that the spring component is linear for the range of operation of strain (small amount of strains). Otherwise, this assumption will be incorrect as the sheet is not a linear spring, and it will not behave linearly for large strains.

Hooke’s law states that

$$f_{spring} = A\sigma_{Hooke} \quad (35)$$

which can be expanded to

$$f_{spring} = AY(\alpha - 1) = yz_0Y(\alpha - 1) \quad (36)$$

$f_{maxwell}$ is the force created when applying a voltage u (related to the charge q):

$$f_{maxwell} = A_{yz}\sigma_m = yz\frac{1}{C_0V}\frac{q^2}{\alpha^2} \quad (37)$$

$$f_{maxwell} = y\frac{z_0}{\alpha}\frac{1}{C_0V}\frac{q^2}{\alpha^2} = \frac{yz_0}{C_0V}\frac{q^2}{\alpha^3} \quad (38)$$

Insert Eqs. 33–37 into Eq. 32 to get

$$mx_0\frac{d^2\alpha}{dt^2} + \gamma x_0\frac{d\alpha}{dt} + yz_0Y(\alpha - 1) - mg = \frac{yz_0}{C_0V}\frac{q^2}{\alpha^3}. \quad (39)$$

Recalling Eq. 19,

$$\frac{1}{C}q = u(t) \Leftrightarrow q = Cu(t) = C_0\alpha^2u(t) \quad (40)$$

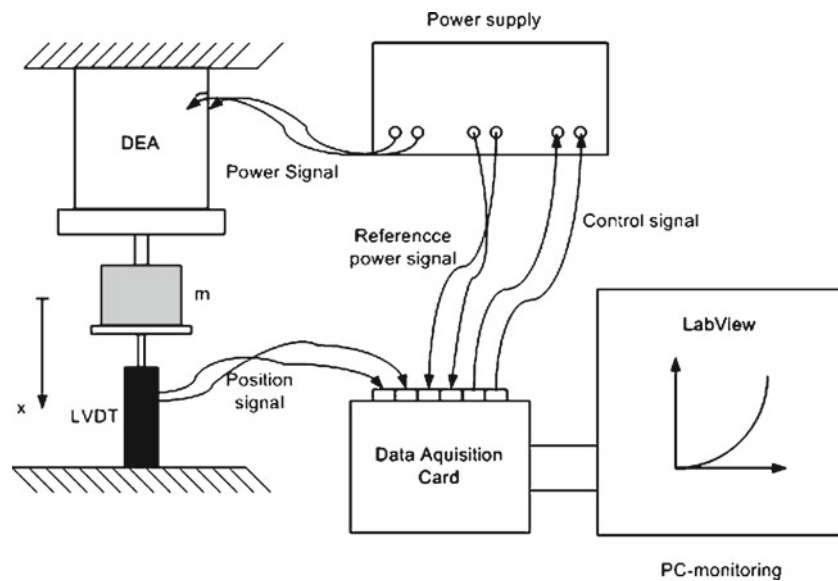
insert this into Eq. 38 to get

$$mx_0\frac{d^2\alpha}{dt^2} + \gamma x_0\frac{d\alpha}{dt} + yz_0Y(\alpha - 1) - mg = \frac{yz_0}{C_0V}\frac{(C_0\alpha^2u(t))^2}{\alpha^3}. \quad (41)$$

Reduce Eq. 41 to get

$$mx_0\frac{d^2\alpha}{dt^2} + \gamma x_0\frac{d\alpha}{dt} + yz_0Y(\alpha - 1) - mg = \frac{yz_0C_0}{V}u(t)^2\alpha. \quad (42)$$

Fig. 6 DEAP dynamic analysis experimental setup



3.4 Approximations

Since α is defined by

$$\alpha = e + 1 \tag{43}$$

the governing equation can be rewritten using Eq. 42 as follows:

$$\begin{aligned} mx_0 \frac{d^2(e + 1)}{dt^2} + \gamma x_0 \frac{d(e + 1)}{dt} + yz_0 Y((e + 1) - 1) - mg \\ = \frac{yz_0 C_0}{V} u(t)^2 (e + 1) \end{aligned} \tag{44}$$

The following system can be reduced to

$$\begin{aligned} mx_0 \frac{d^2(e)}{dt^2} + \gamma x_0 \frac{d(e)}{dt} + yz_0 Y e - mg \\ = \frac{yz_0 C_0}{V} u(t)^2 (e + 1) \end{aligned} \tag{45}$$

simplifying one more step in the strain in common to become

$$\begin{aligned} mx_0 \frac{d^2(e)}{dt^2} + \gamma x_0 \frac{d(e)}{dt} + \left(yz_0 Y - \frac{yz_0 C_0}{V} u(t)^2 \right) e - mg \\ = \frac{yz_0 C_0}{V} u(t)^2. \end{aligned} \tag{46}$$

In order to reduce the complexity of the dynamics governing equations, the assumption shown in Eq. 46 will be applied. The following assumption will be verified later in the experiments section.

$$yz_0 Y \gg \frac{yz_0 C_0}{V} u(t)^2 \tag{47}$$

Concluding the final form of the system governing equations, we have

$$mx_0 \frac{d^2(e)}{dt^2} + \gamma x_0 \frac{d(e)}{dt} + yz_0 Y e = mg + \frac{yz_0 C_0}{V} u(t)^2. \tag{48}$$

4 Testing preparation

4.1 Experimental setup

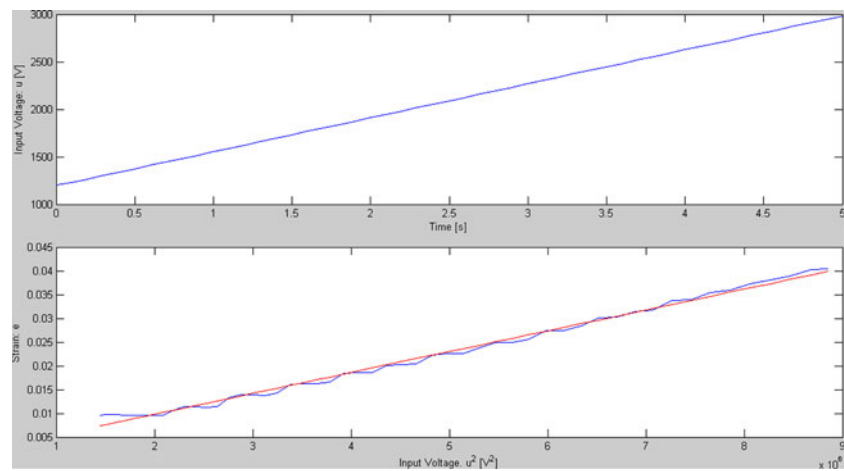
The developed setup used for finding the material properties as well as the dynamic analysis is illustrated in Fig. 6.

In this setup, the DEAP actuator is supplied with the high-voltage signal using a Stanford Research Systems PS 350/5000V-25W amplifier, which is controlled by the program with the help of national instruments data

Table 1 Actuator parameters

Attribute	Unit	Value
ϵ_0	–	8.8542×10^{10}
ϵ_r	–	2.733
m	kg	0.1
C_0	nF	132
y	m	1.875
V	m^3	2.76×10^{-5}
x_0	m	0.184
Y	Pa	9.795×10^5
γ	Ns/m	1

Fig. 7 Top graph ramp input voltage. Bottom graph experimental data showing the strain versus input voltage with a straight line fit



acquisition card (NI 6211). This card also read the signal from the linear variable differential transformer (LVDT) which is a cylinder for linear distance precision measurement over its calibrated range ± 50 mm. The LVDT is attached to the mass to measure the displacement or elongation of the DEAP actuator. The data feed to the amplifier, and the data from LVDT are saved in files that will be used later for analyzing. The collected data as well as the control is allowed using LabView program done for this purpose.

4.2 Material properties

In order to validate the dynamic Eq. 48, it is pre-requested to determine the constants in the equation which represent the DEAP material properties. These are collected in Table 1.

Measurement I - determining the initial length The initial length x_0 is the sum of the unstrained active

length L_0 and the elongation Δx_{mg} when a mass is attached:

Therefore the initial length can be found as follows:

$$x_0 = L_0 + \Delta x_{mg} = 0.180 + 0.004 = 0.184m. \quad (49)$$

Note that the mass is chosen to elongate the material 10 %

Measurement II - determine the Young's modulus Y Recall Eq. 16 which is applicable for small strains (<10 %)

The measurement has been conducted with an input voltage u which is varied as a ramp signal. The elongation Δx is measured using LVDT.

By plotting u^2 versus $\frac{\Delta x}{x_0}$ for a selected range of 1,250–3,000 V, the following range is selected to insure linear strain behavior. Afterward, simulation tool like Matlab is used to calculate the slope α which is the stretch ratio of the material. Note, here, that the stretch

Fig. 8 Fitting the simulation to experiment data by varying the damp factor $\gamma = 1$

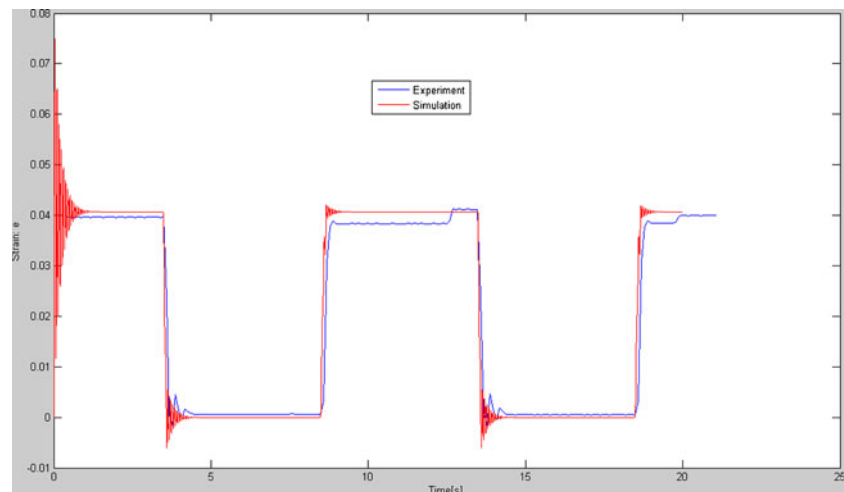
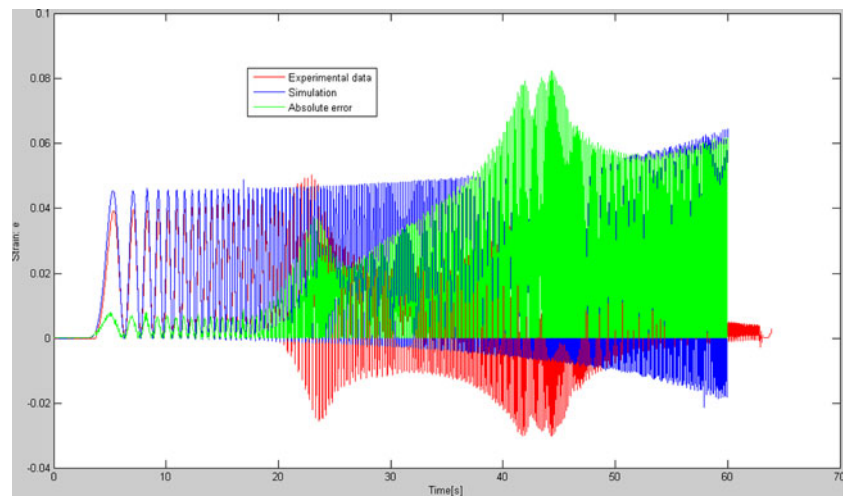


Fig. 9 Testing results showing **a** experimental data in red, **b** model simulation in blue, and **c** absolute error in green. Remark: the input signal $u(t)$ for the simulation and the experiments is the same, whereby the frequency is increased by a factor of 2 as a function of time



ratio can be found with the mechanical Eq. 23 or by the electrical equation, as will be introduced later. The input signal as well as the DEAP strain output is presented in Fig. 7.

Here, the stretch ratio α is defined by using Hooke's law:

$$\alpha = \frac{\epsilon_r \epsilon_0}{z_0^2 Y} \quad (50)$$

from which the Young's modulus can be determined using the parameters stated in Table 1.

$$Y = \frac{\epsilon_r \epsilon_0}{\alpha z_0^2} = 9.795 \times 10^5. \quad (51)$$

Measurement III - determining the damping constant

Recall Eq. 48 a simulation program, Simulink, is used where a step input voltage from the experiment as the input signal is set. All constants are known, except the

damping constant γ , so the damping constant will be tuned until the damping characteristics match with the ones collected from the measurements, as shown in Fig. 8.

It can be noticed that the oscillation frequency is quite different between the measurement and simulation. The frequency is lower in the experiment than predicted by the model. From this, one can also predict that the resonance will happen at a lower frequency in the experiment than that given by the model. The method of determining the damping constant here is not accurate but provide a close approximation.

At the end of this section, Table 1 summarizes the parameters used before conducting the dynamic analysis. Note that the following parameters are found through a set of experiments which is discussed briefly in the testing section as well as the specification supplied from Danfoss PolyPower A/S.

Fig. 10 Zooming into the drift showing the misbehavior of the model closely to the natural frequency

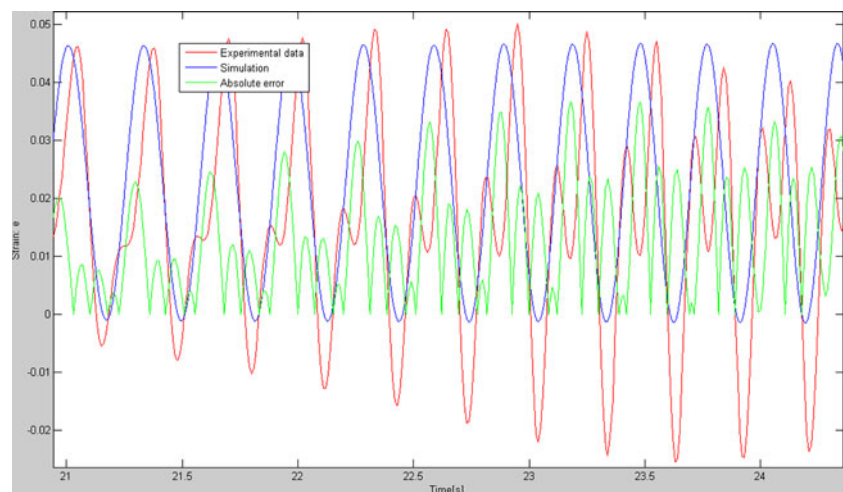
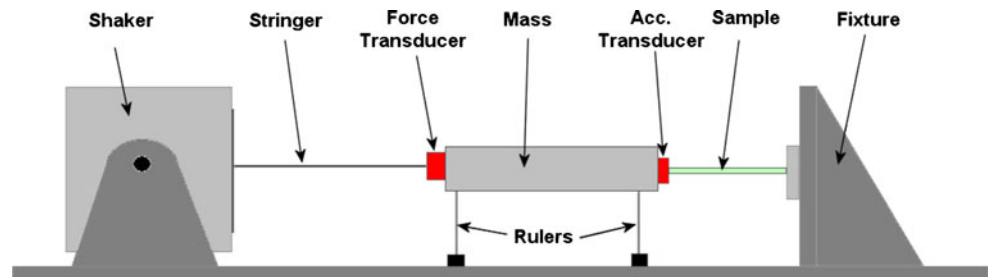


Fig. 11 Shaker concept which can be used to characterize the DEAP film dynamics



5 Results

5.1 Approximations testing

The integrity of the dynamic model can be validated and highly trusted as long as the assumed approximations are verified. So based on that, the validity of the approximations when deriving the final form for the dynamic model, as stated in the governing Eq. 48 has to be checked.

Recalling Eq. 47, based on that, the maximum value of the RHS is

$$\frac{yz_0 C_0}{V} u(t)^2 = 6.5 \quad (52)$$

and of the LHS becomes

$$yz_0 Y = 146 \quad (53)$$

which prove that the undertaken approximation is valid.

5.2 Model validation

The solution for the dynamic model can be validated at this stage, as all the constants of Eq. 48 are determined. Again, Simulink is used to solve the Eq. 48 for a given input signal $u(t)$. This signal is the same as the one applied to the DEAP actuator in the experiment. Based on that, direct comparison can be done in order to determine the precision of the assumption which are later fed in the model. The validation results are shown in Fig. 9.

As can be seen in Fig. 9, for the full range where the model loses its precision, the model as expected does not tend to fit the experimental data quite well in the lower frequency and becomes totally unjustified for the higher frequencies. Moreover, the output amplitude is smaller than the model. This certainly is due to the static friction in the testing rig mainly by the LVDT. It is very important as well to remember the very fundamental of creep in the material which should, in principle, correct some of the losses.

Zooming into the results, as it can be shown in Fig. 10, at about 21 s, the experiment data start to have more than one frequency, and the amplitude is getting larger. This is due to system resonance. At higher frequency, the amplitude of the experiment data is getting smaller.

6 Dynamic analysis alternative methodologies

Two distinct measurement methodologies are described by international norms on how to determine the dynamic characteristics of elastomers [14], direct and indirect [15]. In the direct method, the elastomer is mounted direct to a load cell, exciting the elastomers, and a displacement or acceleration transducer measures the response. The direct measuring method cannot be used at frequencies above 200 Hz. For the indirect method, the elastomer is mounted between two rigid masses, and only the accelerations of these masses are analyzed. The indirect measuring method is used in this project since there have been good results from using this testing method previously. Since the ESA actuator is a thin sheet of electroactive composite and do not support itself, the sample must be pre-strained. This pre-strain must easily and accurately be changeable.

The mounting of the sample should be made, so other sample sizes can easily be measured. The amplitude of the vibration should not exceed that of the designed maximal strain of the sample. The problem with mass loading can be solved by using a stringer used shaker [16] or by carefully selecting the shaker so that the mass loading effect is as small as possible. In this work, a testing rig will be developed in order to perform the dynamic analysis, see Fig. 11.

7 Conclusion

This work addresses the experimental characteristics, mathematical modeling, and model verification for the DEAP fundamental sheet. A range of experiments were carried out using the DEAP film, the material

which can be used to construct the actuators, sensors, and transducers.

The static analysis and the dynamics analysis which can be used to determine as well the steady state voltage–strain characteristics. In addition, the material characteristics were determined (Young’s modulus and the damping constant). These values were later used to validate the dynamic model.

The system results shows a far correlation between the model and the system outputs. This is mainly due to friction and, more important, the creep (or relaxation), whereby the strain would initially reach a value under the step input voltage and then slowly creep toward another point while the input is held constant. This effect is due to the viscoelastic property inherent in any polymer.

Design of the mechanical system is the key as the DEAP sheet material has a low impact on the system dynamics. In this work, the error can be minimized by picking the right range of frequency within 0–20 Hz and, consequently, the system behaviors are improved in this range of frequencies.

Future work includes determining the creep, dynamic hysteresis characteristics, which will be further used in designing optimal position control algorithm.

Acknowledgements The authors would like to thank the engineering staff at Danfoss PolyPower A/S, Nordborg, Denmark for supplying us with the adequate material which enabled us to achieve the goal of studying and identifying the static and dynamic characteristics of the dielectric electroactive polymer material. Moreover, special thanks to Michael Tryson for supplying us with valuable knowledge in the area of conceptualizing the testing rig and handling the material. His dedication to this work is highly appreciated.

References

- Shahinpoor M, Bar-Cohen Y, Simpson J, Smith J (1998) Ionic polymer-metal composites (ipmcs) as biomimetic sensors, actuators and artificial muscles—a review. *Smart Mater Struct* 7:R15–R30
- Attia U, Alcock J (2010) Integration of functionality into polymer-based microfluidic devices produced by high-volume micro-moulding techniques. *Int J Adv Manuf Technol* 48:973–991
- Griffiths C, Bigot S, Brousseau E, Worgull M, Hecke M (2010) Investigation of polymer inserts as prototyping tooling for micro injection moulding. *Int J Adv Manuf Technol* 47:111–123
- Pelrine R, Kornbluh R, Joseph J (1998) Electrostriction of polymer dielectrics with compliant electrodes as a means of actuation. *Sens actuators A Phys* 64(1):77–85
- Bay L, Jacobsen T, Skaarup S, West K (2001) Mechanism of actuation in conducting polymers: osmotic expansion. *J Phys Chem B* 105(36):8492–8497
- Sommer-Larsen P, Hooker J, Kofod G, West K, Benslimane M, Gravesen P (2001) Response of dielectric elastomer actuators. *Proc SPIE* 4329:157–163
- Bar-Cohen Y (2001) Electroactive polymers as artificial muscles—reality and challenges. In: *Proceedings of the 42nd AIAA structures, structural dynamics, and materials conference (SDM)*, Seattle WA, 16–19 April 2001
- Bar-Cohen Y (2004) *Electroactive polymer (EAP) actuators as artificial muscles: reality, potential, and challenges*, 2nd edn. SPIE Press Book, ISBN: 9780819452979
- Brochu P, Pei Q (2010) Advances in dielectric elastomers for actuators and artificial muscles. *Macromol Rapid Commun* 31(1):10–36
- Pelrine R, Sommer-Larsen P, Kornbluh R, Heydt R, Kofod G, Pei Q, Gravesen P (2001) Applications of dielectric elastomer actuators. *Proc SPIE* 4329:335–349
- Bar-Cohen Y (2000) Electroactive polymers as artificial muscles—capabilities, potentials and challenges. *Handbook on Biomimetics* 11(8):1–3
- Madden J, Vandesteeg N, Anquetil P, Madden P, Takshi A, Pytel R, Lafontaine S, Wieringa P, Hunter I (2004) Artificial muscle technology: physical principles and naval prospects. *IEEE J Oceanic Eng* 29(3):706–728
- Iskandarani Y, Jones R, Villumsen E (2009) Modeling and experimental verification of a dielectric polymer energy scavenging cycle. *Proc SPIE* 7287:72871Y
- Petrone F, Lacagnina M, Scionti M (2004) Dynamic characterization of elastomers and identification with rheological models. *J Sound Vib* 271(1–2):339–363
- Carpi F, Chiarelli P, Mazzoldi A, De Rossi D (2003) Electro-mechanical characterisation of dielectric elastomer planar actuators: comparative evaluation of different electrode materials and different counterloads. *Sens Actuators A Phys* 107(1):85–95
- Saldarriaga M, Steffen V Jr, Santos I (2006) Theoretical and experimental analysis of a viscoelastic vibration absorber in a frequency band. *Adv Vib Control Diagn* 205–216